15th World Congress on Computational Mechanics (WCCM-XV)
8th Asian Pacific Congress on Computational Mechanics (APCOM-VIII)
Virtual Congress: 31 July – 5 August 2022
S. Koshizuka (Ed.)

LATERAL RESISTANCE OF BURIED PIPES BY FRICTIONAL LIMIT ANALYSIS

FABIO C. FIGUEIREDO[1*], LAVINIA A. BORGES[1], LUIZ FELIPE MOREIRA[1]

[1] UFRJ - Federal University of Rio de Janeiro, DEM, Av. Horácio de Macedo, 2030 – Ilha do Fundão – Centro de Tecnologia – bloco G-sl.201,Rio de Janeiro, RJ, Brazil
fabiofigueiredo@mecanica.ufrj.br

Key words: Burried pipes, Limit Analysis, Friction, Porous materials

Abstract. *Pipelines are vital means of transportation of liquids and gases over large geographical areas. Regarding buried pipes, they are submitted to thermal and mechanical loads due to their support conditions, pipe-soil friction and the surrounding soil mass. Under high compressive loads carried out by these efforts, loss of stability and buckling may occur. Then, the evaluation of soil lateral resistance that will cause a imminent breakout is important. This work aims the analysis of the soil lateral resistance by frictional limit analysis formulation, considering the soil mass as a deformable body and the pipe as a rigid one. An yield function considering material porosity and material friction angle is considered. The soil lateral resistance forces obtained from the proposed formulation are compared to a those ones considering the limit analysis lower bound found in literature. The fully bounded condition observed in most models is also discussed.*

1 INTRODUCTION

Pipelines are slender structures used for transportation of liquids and gases over large distances. Regarding oil industries applications, in-service hydrocarbons must be transported at hight temperatures and pressure in order to avoid wax formation. Due to expansion resistance, large compressive loads are developed due to thermal stresses, internal pressure and longitudinal friction. If this compressive load overcomes a critical load, sudden large deformation may occur due to loss of stability. The occurrence of buckling depends on soil resistance and friction at pipe-soil interface and the determination of lateral resistance is a key point in order to prevent a sudden failure that can result in economical, environmental and life losses.

Many authors have conducted experimental, analytical and numerical solutions regarding the determination of the lateral resistance on pipes in shallow embedment as found in [1, 2, 3, 4], among others. However, few researches have dealt with finding the lateral resistance of buried pipes and papers in literature are quite limited. In [5], lateral resistance of buried pipes are evaluated by finite elements and limit analysis lower bound. Results considering the soil as a von Mises and Mohr-Coulomb material are presented. In [6], a limit analysis approach is applied in the analysis of buried pipeline submitted to a downward load and [7] shows a experimental procedure and a finite element model for sand and clay soils.

In this work, the lateral resistance is evaluated by frictional limit analysis methodology proposed in [8, 9]. This approach involves contact mechanics, considering permanent contact between a rigid and a deformable body is considered and Coulomb sliding law. Due to a large stiffness ratio between the pipe

and the soil, the pipe is considered as a rigid body while the soil mass is treated as a deformable one. The soil mass is discretized into finite elements and the domain set up in order to accommodate the shear zones and the velocity field. Assuming permanent and known contact region, the pipe-soil interaction is modeled according to frictional unilateral contact conditions. Imposing a lateral velocity field at contact region in order to model the pipe lateral movement, the collapse power, the stress and velocity fields are determined as well as the contact stresses and tangential velocities and the failure modes represented by the slip lines along the soil mass.

In this preliminary study, the soil mass is considered as a von Mises material and compared to a lower bound solution found in literature. Then, a yield criterion considering soil porosity is applied, the called Ulm-Cariou-Gathier (UCG) yield function [10, 11, 12]. If material concentration tends to unity, the UCG yield function tends to Drucker-Prager criterion. The use of this function instead of Drucker-Prager is convenient in order to circumvent its singularity and then providing a family of regular strength criteria that asymptotically tend to the Drucker-Prager criterion [12]. Results considering the soil as a von Mises material and the regularized Drucker-Prager criteria are compared to a lower-bound solution found in [5]. The hypothesis of fully bounded contact is discussed by solving the pipe-soil contact problem and the soil porosity is considered in the analysis.

2 LIMIT ANALYSIS THEORY

Limit analysis aims the determination of a limit state that will entail the incipient plastic collapse for elastic perfectly plastic bodies. The classical limit analysis principles are found in [13, 15]. In order to simulate the lateral resistance problem, the limit analysis approach considering frictional interface proposed in [8, 9] is applied. This methodology considers elements of contact mechanics and instead forces, a velocity field is imposed in order to represent the action of a rigid body onto a deformable one. Permanent contact between the rigid and the deformable body is admitted so as to keep the process ongoing and Coulomb friction law is considered as a sliding law. Concepts of contact mechanics found in [16, 17] are considered in this proposed limit analysis formulation.

The solution technique relies on the discretization of the continuum media is into finite elements and the solution of the discretized mixed limit analysis formulation. Triangular elements are used, with quadratic interpolation for the velocity field and linear interpolation for the stress field [18]. The solver code is implemented in Fortran, based on an iterative procedure based on Newton algorithm and contraction techniques in order to keep the plastic admissibility on the stress field [19]. The set of optimum equations derived from the min-max problem are solved. Then, after a sequence of substitutions and application of a condensation technique, a Linear Complementarity Problem at contact is derived and solved by Lemke algorithm [20, 21]. As results, the plastic collapse power, the stress and velocity fields, the shear zones, normal and tangential forces at contact are determined.

2.1 Kinematics

First, let define a deformable continuum body $\mathcal{B}$ with an imminent contact with a rigid body $\mathcal{B}_r$. Also, let Γ_D and Γ_c be a part of the boundary Γ in which homogeneous and non-homogeneous velocities are imposed, respectively:

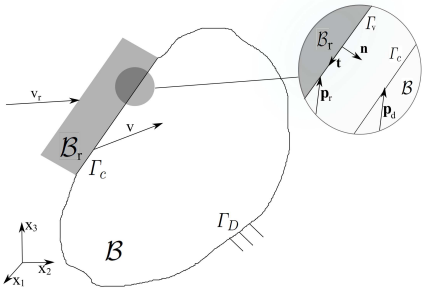

Figure 1: Continuum deformable body $\mathcal{B}$ in imminent contact with the rigid body $\mathcal{B}_r$. In detail, $\mathbf{p}_r$ and $\mathbf{p}_d$ are the position vectors of points on the rigid and deformable bodies at imminent contact.

Now, let define the space V^0 of all kinematically admissible velocity field $\mathbf{v}$ that satisfied the homogeneous boundary conditions on boundary Γ_D:

$$V^0 = \{\mathbf{v} \in \mathcal{U} \mid \mathbf{v} = 0 \quad \text{in } \Gamma_D\} \tag{1}$$

where $\mathcal{U}$ is the space of sufficient regular velocities.

Also, one defines V as an affine space of V^0 [22]. It constitutes the function space of all kinematically admissible velocity fields $\mathbf{v}$ satisfying the homogeneous boundary conditions on Γ_D part of Γ and non-homogeneous boundary conditions at Γ_c:

$$V = \mathbf{v}_p + V^0 \tag{2}$$

where $\mathbf{v}_p$ is a prescribed velocity field.

The strain rate $\mathbf{d}$ that belongs to the set W is related to the velocity $\mathbf{v} \in V$ through the deformation operator $\mathcal{D}$ as follows:

$$\mathbf{d} = \mathcal{D}\mathbf{v}, \qquad \mathbf{v} \in V \tag{3}$$

The kinematics of contact mechanics consists of unilateral conditions at normal direction and a sliding law for the tangential direction. In limit analysis, once incipient plastic collapse is attained, permanent contact hypothesis is assumed. This condition is achieved by setting null the normal gap $g_n = \mathbf{g}.\mathbf{n}$ [23, 24]. Additionally, this conditions is ensured if the normal relative velocity w_n between the deformable and rigid bodies is null. Since separation is not admitted, the Signorini conditions [25] are particularized as follows:

$$w_n = 0,\ r_n < 0,\ r_n w_n = 0 \tag{4}$$

At tangential direction, the relative velocity w_t is defined as the difference $w_t = v_t - v_{rt}$. There is no restriction at this direction and sliding or sticking may occur. Then, a sliding law is required. Denoting the Coulomb friction function as $\mathcal{F}(\mathbf{r}_t, r_n)$ [26, 27, 28], it follows that:

$$\mathcal{F}(\mathbf{r}_t, r_n) = ||\mathbf{r}_t|| + \mu r_n \leq 0 \tag{5}$$

The Coulomb friction law states the occurrence of sliding or sticking regimes:

$$\text{If } \mathcal{F}(\mathbf{r}_t, r_n) = 0, \text{ then } \mathbf{w}_t = -\xi \frac{\partial \mathcal{F}(\mathbf{r}_t, r_n)}{\partial r_t} \tag{6}$$

$$\text{else }, \mathbf{w}_t = \mathbf{0} \tag{7}$$

$$\text{and the complementarity relation:} \tag{8}$$

$$\mathcal{F}(\mathbf{r}_t, r_n) w_t = 0 \tag{9}$$

where: $\mathbf{r}_t = r_t \mathbf{t}$, $r_n < 0$, $\xi \geq 0$ is a proportionally constant and μ is the friction coefficient.

2.2 Equilibrium

The equilibrium between external and internal efforts is posed in terms of the principle of virtual power (PVP), according to [29]. Let $W^{'}$ and W denoting the spaces of stress and strain rate fields, respectively. Considering kinematic in (3), the internal power for any pair $\sigma \in W'$ and $\mathbf{d} \in W$ is defined by the duality product:

$$\langle \sigma, \mathcal{D}\mathbf{v} \rangle = \int_{\mathcal{B}} \sigma \cdot \mathcal{D}\mathbf{v} \, d\mathcal{B}, \quad \mathbf{v} \in V \tag{10}$$

Dissimilar to problems with conventional supports, the PVP considering reaction forces at contact boundary Γ_c is applied as follows [29]:

$$\langle \sigma, \mathcal{D}\mathbf{v}^0 \rangle = \langle \mathbf{a}, \mathbf{v}^0 \rangle_{\Gamma_t} + \langle \mathbf{r}, \mathbf{v}_c^0 \rangle_{\Gamma_c} \tag{11}$$

where: $\mathbf{v}^0 \in V^0$, $\mathbf{v}_c^0 \in V^0$ are velocities at contact boundary Γ_c. Active forces are not imposed in this formulation: $\mathbf{a} = \mathbf{0}$.

Using (2) and considering the hypothesis of permanent contact ($\mathbf{w}_n = \mathbf{0}$), the equilibrium equation is established, according to [9]:

$$\langle \sigma \mathbf{n}, \mathbf{v}_r \rangle_{\Gamma_c} = \langle \sigma, \mathcal{D}\mathbf{v} \rangle - \langle \mathbf{r}_t, \mathbf{w}_t \rangle_{\Gamma_c} \tag{12}$$

where: $\Pi_e = \langle \sigma \mathbf{n}, \mathbf{v}_r \rangle_{\Gamma_c}$ is the external power, $\mathbf{v}_r$ is the velocity of the rigid body and the term related to normal direction was suppressed since $r_n w_n = 0$ according to the complementarity of the unilateral conditions from (4).

2.3 Constitutive

First, let define P as the set of admissible stress field:

$$P = \{ \sigma \in P \mid f(\sigma) \leq 0 \text{ in } \mathcal{B} \} \tag{13}$$

where: $f(\sigma)$ is the yield function.

In order to relate strain rates and stress fields, the normality law derived from Hill's maximum dissipation principle and based on subdifferential of plastic dissipation function $\chi(\mathbf{d}^p)$ is defined as follows ([13, 14]):

$$\chi(\mathbf{d}^p) = \sup_{\sigma^* \in P} \langle \sigma^*, \mathbf{d}^p \rangle \tag{14}$$

The normality law is a consequence of this principle. Admitting the existence of a convex set P it follows:

$$\mathbf{d}^p = \dot{\lambda}\nabla f(\sigma), \tag{15}$$

$$f(\sigma)\dot{\lambda} = 0 \quad \dot{\lambda} \geq 0, \quad f(\sigma) \leq 0 \tag{16}$$

2.4 Limit analysis formulation

The aim of limit analysis consists in finding the external collapse power Π_e that will entail the incipient plastic collapse under permanent regime configuration, the stress field $\sigma \in P$ that satisfied the equilibrium in (12), the kinematically admissible velocity $\mathbf{v} \in V$, the strain rate field $\mathbf{d}^p$ related to the velocity field $\mathbf{v}$ through equation (3).

The solution scheme is based on discrete form of the limit analysis formulation stated in [8, 9]. The velocity and stress fields are quadratic and linearly interpolated, respectively. Considering the discrete form the strain operator as $\mathbf{B}$ ([19, 18]), the discrete form of the mixed limit analysis formulation is derived as follows:

$$\Pi_e = \min_{\mathbf{v},\mathbf{w}_t} \max_{\sigma,\mathbf{r}_t} (\sigma \cdot \mathbf{B}\mathbf{v} - \mathbf{r}_t \cdot \mathbf{w}_t) \tag{17}$$

such that :

$$\mathbf{f}(\sigma) \leq \mathbf{0} \text{ in } \mathcal{B} \tag{18}$$

$$\mathcal{F}(\mathbf{r}_t, r_n) \leq \mathbf{0} \text{ at } \Gamma_c \tag{19}$$

$$\mathbf{w}_n = \mathbf{0} \text{ at } \Gamma_c \tag{20}$$

The solution of the above optimization problem with constraints is based on a Newton algorithm as described in [19, 18] and [9]. From solution, the collapse power (associated with cutting forces), the velocity and stress fields, reaction forces and the plastic multiplier are determined.

2.5 Yield function

As it is well known, soils are heterogeneous materials composed of porous and solid particles. Porous may be totally or partially filled with water. In these conditions there are a large number of possible loading and boundary conditions in geotechnical problems.

From a microscopic point of view, soils are composed of a mix of lots of different particles, creating a very heterogeneous material. Because of its heterogeneity and presence of porous, the determination of mechanical properties of such materials becomes a difficult task. In order to solve this, the development of a predictive model to determine the strength of porous materials will make extensive use of the theory of strength homogenization. Recent advances on homogenization techniques are found in [12].

Porous materials with a dominating matrix-pore inclusion morphology are well represented by the Mori-Tanaka and Self-Consistent schemes, as seen in [12] and [11]. In Mori-Tanaka scheme some material parameters such as $\alpha_d, \sigma_0, \alpha_m$ are calculated and they include the soil cohesion, porosity and friction angle effects. The called Ulm-Gathier-Cariou (UGC) yield function is written in Equation (21):

$$F(J_2,\Sigma_m) = \left(\frac{\Sigma_m + \sigma_0}{\alpha_m}\right)^2 + \left(\frac{J_2}{\alpha_d}\right)^2 - 1 \tag{21}$$

where $\alpha_d, \sigma_0, \alpha_m$ are material parameters and calculated as seen in [12] and [11], the second invariant J_2 is associated to deviatory stress and Σ_m is mean stress.

Depending on density packing value η defined in Equation (22), the UGC yield function may assume and elliptical or an hyperbolical shape:

$$\eta = \frac{V_s}{V_t} \tag{22}$$

where V_s is the solid volume and V_t is the material total volume, including pores.

Mori-Tanaka morphology is applied in this work and according to it, there is a density packing critical value that defines two distinct regimes: below the critical value, the yield function assumes the elliptical shape; otherwise, it assumes the hyperbolical shape. This critical density packing η_{crit} is function of friction angle α_s and calculated as in Equation (23):

$$\eta_{crit} = 1 - \frac{4\alpha_s^2}{3} \tag{23}$$

Moreover, under certain special conditions, the UGC function may reach asymptotically either to von Mises or Drucker-Prager criteria: von Mises criterion is obtained if friction angle $\alpha_s \to 0$ and packing density $\eta \to 1$; however, if $\alpha_s \neq 0$ and $\eta = 1$, Drucker-Prager criterion is obtained.

Figure 2 shows an example of UGC function, plotting J_2 (deviatory) versus σ_m (mean stress) for a friction angle $\alpha_s = 0.4$. In this case, $\eta_{crit} = 0.786$ and it means that any packing density below this critical value, the yield surface has an elliptical shape and otherwise, the criterion is hyperbolical. It is also observed that when $\eta \to 1$ the cone-shaped Drucker-Prager criterion is reached. If von Mises citerion were represented, it would be an horizontal line parallel to mean stress axis since Mises is independent of the mean stress, as expected.

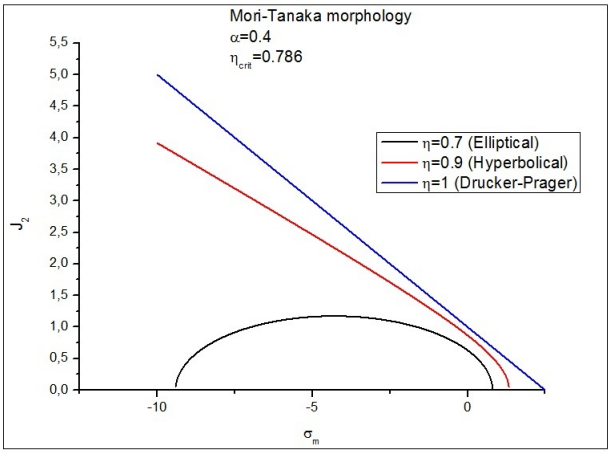

Figure 2: Yield function regimes: elliptical below η_{crit}, hyperbolical above this value and limited by Drucker-Prager when $\eta = 1$.

3 ANALYSIS OF BURIED PIPES

A pipe of long length and diameter D is buried at a depth H in a soil mass. Preliminarily, the soil was considered as a von Mises material and the UGC yield function was applied so as to tend to Drucker-Prager, under fully bonded condition. Later, the frictional problem was carried out in order to evaluate the normal stresses around pipe-soil interface. If the restriction for the normal force (stress) condition in (4) is violated, there is loss of contact at some part of pipe-soil interface at imminent plastic collapse.

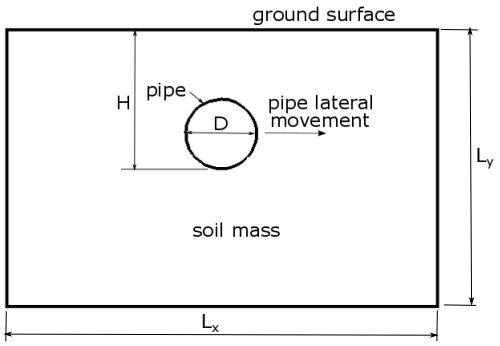

Figure 3: Problem definition for soil lateral resistance evaluation.

In Fig. 4, the dimensions L_x and L_y are defined so that the resulting slip lines and velocity fields are fully contained in the analysis domain. First, in order to compare to the lower-bound solution found in [5], the fully bonded contact between the pipe and the surrounding soil mass is considered. Later, friction is considered at pipe-soil interface and the hypothesis of contact over entire pipe-soil interface is discussed and the effect of soil porosity is evaluated.

3.1 Comparison with a lower-bound solution

First, the soil lateral resistance obtained from the limit analysis formulation in this paper is compared to the lower bound solution found in [5]. In this work, a parametric study was performed by varying the embedment radio H/D and the magnitude of the internal friction angle α_s, from 0^o up to 40^o. Mohr-Coulomb yield criterion was applied to describe the soil behaviour under plasticity. In this approach, the non-dimensional lateral capacity factors F_c and F_γ due to soil cohesion and soil weight were determined, respectively. The fully bonded condition was adopted.

This work presents preliminary results considering von Mises criterion ($\alpha_s = 0^o$). The soil self-weight is not computed. Then, the ultimate load P_u and the lateral resistance are related as follows:

$$P_u = cDF_c \tag{24}$$

where: c is the material cohesion and D is the pipe diameter.

In the present work the self-weight is not computed.

Relating these quantities, the lateral resistance F_c for embedment ratio from 2 up to 10 are compared:

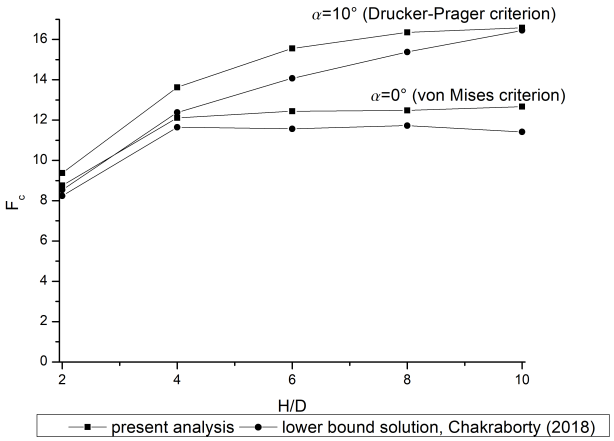

Figure 4: Soil lateral resistance.

One should observe that the present limit analysis is a mixed formulation and the results are compared to a lower bound ones. Due to this dissimilarity, the results do not need to match necessarily. Moreover, Drucker-Prager criterion was implemented in the present while in [5] Mohr-Coulomb was considered.

Later, failure modes regarding the embedment ratios are present as well the velocity field. The following figures are related to $H/D = 2$ ($H/D = 4$ presents a similar result), considering a von Mises and Drucker-Prager material (D-P):

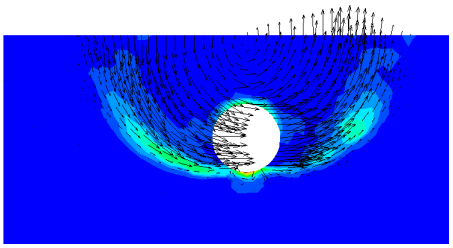

Figure 5: Velocity field and failure mode for a shallow embedment (H/D=2): von Mises material.

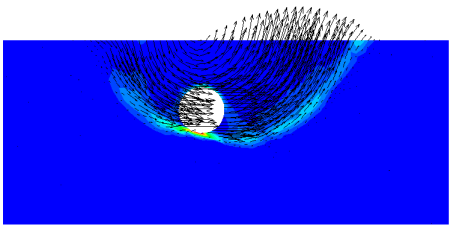

Figure 6: Velocity field and failure mode for a shallow embedment (H/D=2): D-P material ($\alpha_s = 10^o$).

For a deeper embedment ratio $H/D = 8$, the failure modes considering a von Mises and a Drucker-Prager materials are compared:

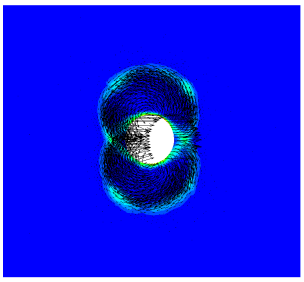

Figure 7: Velocity field and failure mode for a deeper embedment (H/D=8): von Mises material.

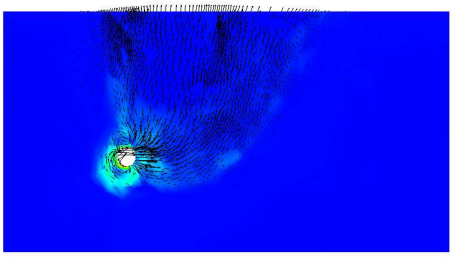

Figure 8: Velocity field and failure mode for a deeper embedment (H/D=8): D-P material ($\alpha_s = 10^o$).

Regarding Figures 5 and 6, the failure modes are similar and they meet the ground surface. In these cases, a depression may occur on the left and a pile on the right of the pipe at collapse. For a deeper embedment ratio, Figure 5 presents a failure mode around the pipe diameter and a material recirculation around it. This failure mode is similar to the deep failure mode found in [6]. However, if a material with internal friction is considered, Figure 8 presents a failure mode with a certain material circulation and some part moves to the upper surface as observed in Figures 5 and 6.

3.2 Pipe-soil frictional analysis

The fully bonded cases analysed so far consider permanent contact and sticking around the pipe-soil interface. The plausibility of this hypothesis can be verified by solving the frictional problem at pipe-soil interface. First, permanent contact was considered at this interface and the normal stresses at contact were evaluated. There is contact if (4) is met. Positive values imply loss of contact. Considering the embedment ratios $H/D = 2$ and $H/D = 6$ and friction coefficients at pipe-soil interface from 0.10 to 0.30, the normal stresses around the contact circumference were plotted as follows:

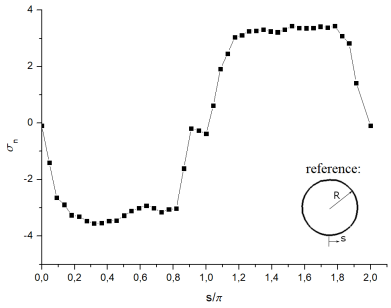

Figure 9: Distribution of contact normal stresses for H/D=2, μ=0.10.

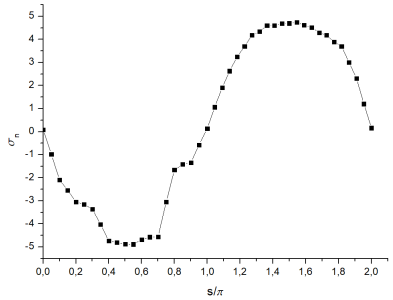

Figure 10: Distribution of contact normal stresses for H/D=6, μ=0.30.

Observing the results in Figures 9 and 10, there are positive normal stresses for $s/\pi > 1$. Then, at imminent plastic collapse there is loss of contact $1 \leq s/\pi \leq 2$ and the fully bonded condition may provide overrated lateral forces. The effective contact shall be $0 \leq s/\pi \leq 1$. The lateral resistances regarding full contact and effective contact are compared as follows:

Table 1: Comparison between full contact x effective contact results for lateral resistance.

μ	H/D	Fc (full contact)	Fc (effective contact)
0.1	2	7.4315	3.9204
0.3	6	10.2190	6.1042

3.3 Frictional porous soil

After validation and analysis of effective pipe-soil contact at plastic collapse, the soil lateral resistance is now evaluated considering soil porosity. The YGC yield function was applied and sticking was considered at pipe-soil interface for $H/D = 4$ and $H/D = 8$. The material friction angle is 10^o and lateral resistance F_c was evaluated for $0.50 \leq \eta \leq 1.0$. Under this condition, the critical density packing is $\eta_{crit} = 0.7672$ according to (23).

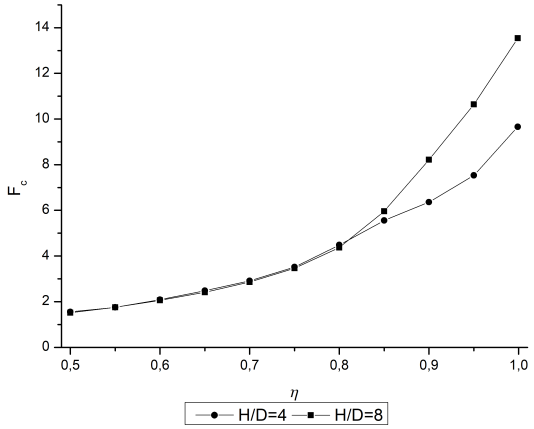

Figure 11: Soil lateral resistance for a porous soil.

Observing Figure 11, as porosity increases, the lateral resistance decreases due to contraction of the space of admissible stresses in UGC yield-function as long as porosity increases. According to theory, there is a critical porosity (or density packing η) in which the UGC yield function changes from hyperbolical to elliptical shape. According to the results, if density packing is bellow the critical point, there is little influence of embedment ratio on evaluation of the lateral forces. This fact should be better investigated by analysing more cases.

4 Conclusions

In this paper, the soil lateral resistance is evaluated by limit analysis theory considering frictional interfaces. In this formulation, the soil is considered as a deformable body while the pipe is treated as a rigid one and the contact between them is supposed known *a priori* and permanent,i.e., separation is not allowed. Under these assumptions, the normality of sliding law based on Coulomb friction is imposed implicitly and friction dissipation is included into the limit analysis formulation.

The proposed formulation was applied in the analysis of lateral resistance of a buried pipe. As a first step, the results concerning fully bonded contact was applied and the soil behavior under plasticity

described by von Mises and Drucker-Prager yield criteria. Drucker-Prager criterion was approximated by UGC yield function by making density packing near 1, implying a little regularization in the criterion. The obtained results for soil lateral resistance were coherent to the lower bound solutions found in [5]. However, higher friction coefficients should be tested in the evaluation of soil lateral resistance.

Considering the soil as a von Mises material two failure modes were observed: for a shallow embedment the slip lines intercepts the ground surface and the occurrence of a deep failure mode. However, for a Drucker-Prager material this distinction was not observed.

After this step, the plausibility of fully bonded hypothesis was verified by solving the limit analysis formulation with frictional interface. According to Signorini unilateral conditions, if there is contact, the normal forces (stresses) at contact should be negative. Then, considering the contact at entire circumference, the distribution of normal stresses were plotted and it was concluded that at imminent plastic collapse, there is contact loss at some part of circumference contact. According to these results, there is an effective contact region and the fully bonded condition may overestimate the soil lateral resistance.

Finally, the soil porosity was considered and some preliminary results were presented. One should regard little or none influence of embedment ratio on evaluation of soil lateral resistance if density packing is bellow the critical value. This behavior should be investigated by testing another embedment ratios. Regarding the algorithm convergence, there is an improvement as long as porosity increases and the UGC yield function becomes elliptical and it departs from Drucker-Prager criterion.

As future work, a limit analysis formulation considering self-weight should be implemented since it plays an important rule on geological problem. The behaviour of soil lateral resistance considering soil porosity as presented in Figure 11 shall be investigated by implementing the soil self-weight.

REFERENCES

[1] Marifield, R. and White, D. and Randolph, M.F. The Ultimate Undrained Resistance of Partially Embedded Pipelines. *Géothechnique* (2008) **58**: 461–470.

[2] Aubeny, C. P. and Shi, H. and Murff, J. D. Collapse Load for Cylinder Embedded in Trench in Cohesive Soil. *International Journal of Geomechanics* (2005) **5**: 320–325.

[3] Randolph, M. F. and White, D. J. Upper-Bound Yield Envelopes for Pipelines as Shallow Embedment in Clay. *Géothechnique* (2008) **58**: 297–301.

[4] Murff, J. and Wagner,A. and Randolph, M.. Pipe Penetration in Cohesive Soil. *Géothechnique* (1989) **39**.

[5] Chakraborty, D. Lateral Resistance of Buried Pipeline in c-ϕ Soil. *Journal of Pipeline Systems Engineering and Practice* (2018) **9**.

[6] Kouretzis, G.P. and Krabbenhøft, K. and Sheng, D. and Sloan, S.W. Soil-buried Pipeline Interaction for Vertical Downwards Relative Offset. *Canadian Geotechnical Journal* (2014) **51**: 1087–1094.

[7] Liu,R., Guo, S. and Yan, S. Study on the Lateral Soil Resistance Acting on the Burried Pipeline. *Journal of Coastal Research* (2015) **73**: 391–398.

[8] Figueiredo,F., Borges, L. Limit Analysis Formulation for Frictional Problems. *Archive of Applied Mechanics* (2017) **86**: 1965–1977.

[9] Figueiredo,F., Borges, L. Limit Analysis and Frictional Contact: Formulation and Numerical Solution. *Meccanica* (2020) **55**: 1347–1363.

[10] Cariou,S., Ulm, F.J. and Dormieux, L. Hardness-packing Density Scaling Relations for Cohesive-frictional porous materials. *Journal of Mechanics and Physics of Solids* (2008) **56**: 924–952.

[11] Cariou, S. *The Effect of the Packing Density on the Indentation Hardness of Cohesive-Frictional Porous Materials*. Ph.D. Thesis, Massachussetts Institute of Technology, (2006).

[12] Gathier, B. *Multi Scale Homogenization - Application to Shale Nanoindentation*. Ph.D. Thesis, Massachussetts Institute of Technology, (2006).

[13] Lubliner, J. *Plasticity Theory*. Pearson Education, (1990).

[14] Maugin, G. *The Thermomechanics of Plasticity and Fracture*. Cambridge University Press, (1992).

[15] Chen, W. F. and Liu, X. L. *Limit Analysis in Soil Mechanics*. Elsevier Science Publishing, (1990).

[16] Wriggers, P. *Computational Contact Mechanics*. John Wiley Sons, (2002).

[17] Weißenfels, C. and Wriggers, P. Methods to Project Plasticity Models onto the Contact Surface Applied to Soil Structure Interactions. *Computers and Geotechnics* (2015) **65**: 187–198.

[18] Zouain, N. and Borges, L. and Silveira, J. L. Quadratic Velocity-Linear Stress Interpolations in Limit Analysis. *International Journal for Numerical Methods in Engineering* (2014) **98**: 469–491.

[19] Borges, L. A. and Zouain, N. and Huespe, A. E. A Nonlinear Optimisation Procedure for Limit Analysis. *European Journal of Mechanics /A Solids* (1996) **15**: 487–512.

[20] Belegundu, A. D. and Chandrupatla, T. R. *Optimization: Concepts and Applications in Engineering*. Cambridge University Press, (2014).

[21] Bazaraa, M. and Sherali, H. D. and Shetty, C. M. *Nonlinear Programming: Theory and Algorithms*. John Wiley Sons, (2006).

[22] Anton, H. and Busby, R. C. *Contemporary Linear Algebra*. John Wiley Sons, (2003).

[23] Wriggers,P. Finite Elements for Thermomechanical Contact and Adaptive Finite Element Analysis of Contact Problems. *CISM Courses and Lectures: New Developments in Contact Problems* (1999) **384**: 177–246.

[24] Chabrand, P. and Dubois, F. and Raous, M. Various Numerical Methods for Solving Unilateral Contact Problems with Friction. *Mathematical and Computer Modelling* (1998) **28**: 97–108.

[25] Panagiotopoulos, P.D. A Nonlinear Programming Approach to the Unilateral Contact and Friction-boundary Value Problem in the Theory of Elasticity. *Ingenieur Archives* (1975) **44**: 421–432.

[26] Raous, M. Quasistatic Signorini Problem with Coulomb Friction and Coupling to Adhesion. *CISM Courses and Lectures: New Developments in Contact Problems* (1999) **44**: 101–178.

[27] Michalowski, R. and Mroz, Z. Associated and Non-associated Sliding Rules in Contact Friction Problems. *Archives of Mechanics* (1978) **30**: 259–276.

[28] Saxcé, G. and Bousshine, L. Limit Analysis Theorems for Implicit Standard Materials: Application to the Unilateral Contact with Dry Friction and the Non-Associated Flow Rules in Soils and Rocks. *International Journal of Mechanical Science* (1998) **40**: 387–398.

[29] Taroco, E. O. and Blanco, P. J. and Feijóo, R. A. *Introducción a la Formulación Variacional de la Mecánica*. LNCC/CNPq, (2017).